The Eurasia Proceedings of Science, Technology, Engineering & Mathematics (EPSTEM)
ISSN: 2602-3199

The Eurasia Proceedings of Science, Technology, Engineering and Mathematics (EPSTEM), 2025

Volume 37, Pages 1082-1096

ICEAT 2025: International Conference on Engineering and Advanced Technology

Impact of Duct Position on Behavior of High-Strength Reinforced Concrete Flat Slab

Mohammed Hammed Al-Khazraji
University of Kufa

Haider Ali Al-Tameemi
University of Kufa

Abstract: Structural and architectural designers consider flat floors as preferable slab systems in medium-rise buildings. The ability of this slab system to incorporating ducts enhancing its functional efficiency. However, incorporated ducts impacting flow of the interior forces and reducing the slab stiffness, most notably when the ducts pass near columns. İn addition to brittle nature of high-strength concrete. Therefore, the shear resistance significantly reduced and the risk of brittle punching failure highly increased. Thus, the main goal was to evaluate the behavior of the punching shear for flat slabs composed of high-strength concrete that incorporates built-in ducts. For this purpose, six two-way slab specimens were fabricated with a duct, and one solid specimen served as a control specimen. Two main parameters were studied: the distance of the duct opening to the face of the column over horizontal distances of 0, 50, and 100 mm for two types of opening (30 × 100 mm) and (50 × 100 mm), and the duct height with two values of 30 and 50 mm. The outcomes indicate that shear behavior was negatively affected as the duct moved closer to the column face and as duct height increased. The ultimate load capacity decreased most at the column face, by up to 42.1%. Serviceability worsened in both parameters of the study, particularly as the duct was closer to the column face and the duct height increased. Additionally, duct deflection increased significantly, and specimens often failed to meet the service load requirements. The toughness generally declined with both closer proximity and greater duct height. The most severe reductions occurred at the 0 mm position, where toughness dropped by over 50% in both 30 mm and 50 mm duct height specimens. All slab specimens, including a solid control specimen, exhibited the exact failure mechanism, known as punching failure.

Keywords: Eco-friendly construction, High-strength concrete, Punching shear, Self-compacting concrete, Two-way shear slab.

Introduction

The flat slab represents a two-way slab with reinforcement, typically without beams or girders, in which columns directly support the slab, transferring loads to columns. Constant-thickness slabs that do not include column capitals or drop panels are commonly referred to as flat plates (Hassoun & Al-Manaseer, 2020). Concrete buildings constructed with flat slabs are a popular type of reinforced concrete structure in the construction field, particularly in medium-height office buildings. The crucial point in the construction of flat slabs made from reinforced concrete is the connection between the column and slab, which ensures adequate deformation and punching shear resistance for the slab in the connection area (Olmati et al., 2017). Over the past few decades, reinforced concrete constructions, including flat slabs, have become a widespread and efficient option for housing and commercial buildings globally due to their numerous advantages (Faria et al., 2020). Utilization systems of flat slabs are also prevalent in schools,

- Selection and peer-review under responsibility of the Organizing Committee of the Conference

hotels, and hospitals. They are fast and straightforward to make mold for concrete casting and building. Utilizing a flat slab will shorten the construction process, as extensive table formwork is used (Dhavale & Fayaz, 2019).

Punching shear failure is a significant concern in flat slabs, particularly due to the high stress concentration around columns, resulting in a brittle, cone-shaped failure with little warning (Lapi et al., 2019; Ghayeb et al., 2023; Said et al., 2020). Once it occurs, the slab-column joint loses all shear capacity, causing sudden slab detachment and posing a severe risk to overall structural stability (Shatarat & Salman, 2022). When the beams are excluded, this results in shorter stories' heights, reducing the costs of various types of construction elements such as cladding, vertical partition walls, mechanical components, and pipes, particularly for medium or high-rise buildings. This permits to conserve approximately 10% of the vertical members and thereby leads to reducing the applied loads on the foundation. Generally, using flat slabs makes it easier to change partition positions and access to service and repair (Kolapuri et al., 2018). On the other hand, there are several structural limitations restricting the using of flat slab systems. The poor transverse stiffness due to missing of shear walls or deep beams, leading to increasing lateral displacements. This can result in damage in the non-structural elements, even due to moderate seismic activity. Furthermore, such slab systems are more susceptible to fail in a brittle punching manner because of shear forces and unbalanced moments transferred directly between slabs and columns.

Over the past two decades, concrete technology has significantly advanced, enabling product mixes exceeding 100 MPa using standard materials (Zhou et al., 1995). High-strength concrete (HSC) is considered as ideal choice for elements subjected to high compressive stress, such as arches, shells, deep beams, and folded plates (Kamonna et al., 2020; Rashid & Mansur, 2009). It allows for reduced cross-sectional areas of the structural elements and thereby minimizing both space and material usage (El-Mawsly et al., 2022). The inclusion of silica fume, which is rich in amorphous SiO_2, leads to enhancing the matrix density and the overall concrete strength, especially when it combined with superplasticisers, as widely reported in the literature (Shannag, 2000). To retain and keep the advantages of flat slab systems, the services of the buildings should be integrated within the slab thickness and thereby eliminating the need for ceiling drops and reducing wasted space (Mehdi & Al-Tameemi, 2024 b; Thiele, 2010). The inclusion of service ducts with the slab thickness supports a more eco-friendly and cost-effective construction approach due to reducing raw material usage and energy consumption, especially in multi-story buildings. Additionally, concrete's thermal mass allows for the incorporation of heating or cooling pipes within the slab (Hanson, 1970). The two-way shear behavior of high-strength reinforced concrete (HSRC) flat slabs with embedded ducts is considered a significant issue in modern multi-story and long-span structures. Although the ducts serve essential mechanical, electrical, and plumbing (MEP)functions, they potentially weakened shear resistance due to disrupting stress distribution and reducing the effective concrete section. Practically, these services are often placed near the slab–column connection in flat slab systems. Although high-strength concrete (HSC) enhances compressive strength, its brittle nature and low post-cracking ductility can further compromise shear performance. Therefore, it is essential to study the effects of duct placement on punching shear capacity and develop appropriate detailing strategies to maintain structural safety and integrity (Al-Tameemi et al., 2021; Al-Bahrani & Al-Tameemi, 2025 b; Al-Quraishi, 2014).

Ghannoum (1998) studied the performance of internal connections between slabs and columns in flat plates. Six specimens of the slab-to-column, which acted in two directions to fail in punching shear, have been discussed. The impact of high-strength concrete on the punching shear capacity was studied. The improvement in punching shear strength of slabs resulting from the utilization of concrete with high strength amounted from 21% to 41% for slabs featuring a uniform top bar distribution, and from 47% to 53% for slabs with banded flexural reinforcement distribution. (Metwally et al., 2008) investigated the performance of flat slabs made of high-strength concrete exposed to punching loads. Analytical studies and experimental investigations were conducted to evaluate the punching shear performance and capacity of both normal- and high-strength flat slabs. They found that increasing concrete strength from 30 to 65 MPa resulted in an increase by 78% in the ultimate load. (Lee & Yoon, 2010) investigated the structural behaviour of connections between a column and a slab constructed using high-strength concrete reinforced with fiber. The primary variable examined involved the implementation of high-strength concrete reinforced with fiber. The findings showed that providing fibre-reinforced concrete with high strength in the slab surrounding the column for a length double the influential depth of the slab, beginning at the face of the column, significantly improves performance. This includes increased compressive strength in the axial direction, greater stiffness, a more even distribution of strains throughout the column, a lower number of small cracks during the entire load stages within the slab, and reduced strains in the transverse direction within the joint between column and slab. (Al-Quraishi, 2014) tested slab-column connections imposed under punching loads, which had been considered concentrated. The impact of the compressive strength of concrete was investigated through tests of six slabs made with ultra-high-performance concrete and one slab made with concrete that has a normal strength. The punching cone diameter for slabs with UHPC was greater than that of slabs with NSC, and the position of the crucial shear crack on the tension surface was further away from the column face. The punching cone angle of slabs made of UHPC was smaller than that of slabs made of NSC. (Yehia et al., 2023) investigated the punching shear behavior of Ultra-High-Performance Concrete (UHPC) experimentally and numerically. The mean test specimen strength ranged from 9.6 to 13.1 MPa in tension and varied from 164 MPa to 193 MPa in compression. The outcomes showed that utilizing UHPC with incorporated steel fibers on a micro-scale in flat slabs altered the punching shear response from an entirely brittle failure in shear to a somewhat ductile one, as demonstrated by an increase in the ductility percentage from 2.77 to 3.57. When UHPC was used in flat slabs, the punching cone diameter was greater relative to that of regular concrete. The raised compressive strength of concrete resulted in a 22.7% and 11.4% increase in load and deflection at (d/2) from columns compared to the other specimens. The most significant increases in initial and ultimate stiffness, as well as the energy absorption values, reached 40.62%, 24.48%, and 41.4%, respectively. (Mehdi & Al-Tameemi, 2024 a) investigated the impact of incorporated pipelines on the performance of punching shear of seven lightweight concrete flat slabs with constant dimensions and varying spacing between the pipelines and the area of loading. The findings demonstrated that the punching shear strength decreases by 28% and 15% for distances of 0 mm and 50 mm, respectively, compared to the control specimen, as the pipeline approaches the loading region. Additionally, high-strength concrete increases this capacity by 25% and 10% at the exact locations, respectively. Utilizing concrete with high strength in the surrounding zone of the pipeline enhanced the punching load capacity immediately adjacent to the loaded area. (Al-Bahrani & Al-Tameemi, 2025 a) explored the effect of using hybrid concrete section on the performance of punching shear of normal concrete flat slabs with inset pipelines. The findings demonstrated that the punching shear strength increases up to 25% due to using higher strength concrete of 48 MPa instead of normal concrete of 25 MPa in the region around the pipeline, compared to the control specimen, Additionally, the use of hybrid section was more effective as the pipeline approached the loaded area. Despite the international building codes having provisions to calculate the punching shear capacity reduction caused by vertical openings in flat slabs, these codes lacked any provisions to forecast the impact of installing embedded ducting lines in flat slabs.

This study presents a novel experimental investigation into the two-way shear behavior of high-strength reinforced concrete flat slabs incorporating embedded ducts within the slab thickness. Unlike previous research, which has primarily focused on conventional concrete or flexural performance, the current work uniquely examines how variations in duct position and height impact punching shear resistance. The integration of service ducts in high-strength concrete slabs introduces complex stress redistributions and potential shear weaknesses that have not been comprehensively studied. The findings offer valuable insights into how the location of constructed ducts affects both the load-carrying capacity and serviceability performance of high-strength flat slabs, thus facilitating the optimal placement of ducts for these applications.

Methodology

Specimens

The specimens used in the current investigation were identical in dimensions. They were measuring 1050 mm × 1050 mm, and their thickness was 100 mm. Each slab specimen was provided with a square shaped steel plate, measuring 100 mm on each side, centered on the top surface. This plate represents the area where the load was applied to simulate a column load action which is a crucial aspect of the present study. All slab specimens were reinforced with the same steel-bars gride for the tension zone. The steel-bars gride contained 10 mm diameter bars in two directions, with a spacing of 60 mm across the bottom portion of the slab, and with a 15 mm concrete cover, as illustrated in (Figure 1). The design of the tested specimens was adhered to the guidelines described in the ACI 2019 code in a such manner that led to avoiding flexural failure and to ensuring appropriate behavior under shear failure caused by punching. (Figure 2) demonstrates the geometry of the duct in the slab. Despite having consistent dimensions and reinforcement arrangements, each slab specimen features distinct geometric configurations form the others. This differentiation was intentional because each specimen was designed to investigate the punching shear performance under a different condition. Specimen coding system was developed to simplify the identification of the distinct characteristics of each specimen. The label system **S.a.b.x** is a systematic naming pattern used to identify slab specimens based on the geometric properties of inbuilt ducts, as demonstrated in (Table 1). In this format, "**S**" denotes a slab specimen, "**a**" represents the duct height in centimeters, "**b**" indicates the duct width in centimeters, and "**x**" specifies the horizontal distance from the column face to the corner of the duct, also in centimeters. (Table 1) clarifies the details of specimens tested according to the present work. A parametric investigation with two variables, including distance from the column face and duct height, explored the behavior in flat slab specimens with built-in ducts. Therefore, the two-way slab specimens were grouped and arranged according to these parameters, as outlined in (Table 1). The first study parameter represented the distance of the duct opening to the face of the column, which included three horizontal distances: 0, 50, and 100 mm. This parameter was studied for the duct sizes of 30 mm × 100 mm and 50 mm × 100 mm. The second parameter represented the column height, with two values of 30 and 50 mm chosen. This parameter was evaluated at two locations from the column face, at 0 mm and 50 mm.

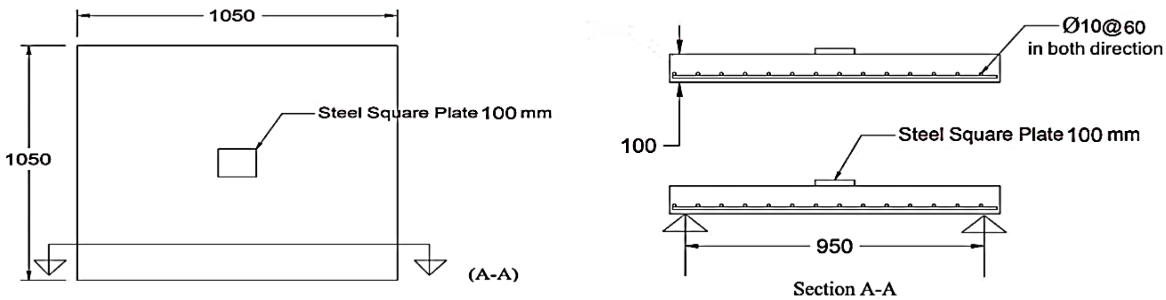

Figure 1. Specimen dimensions and details of reinforcement

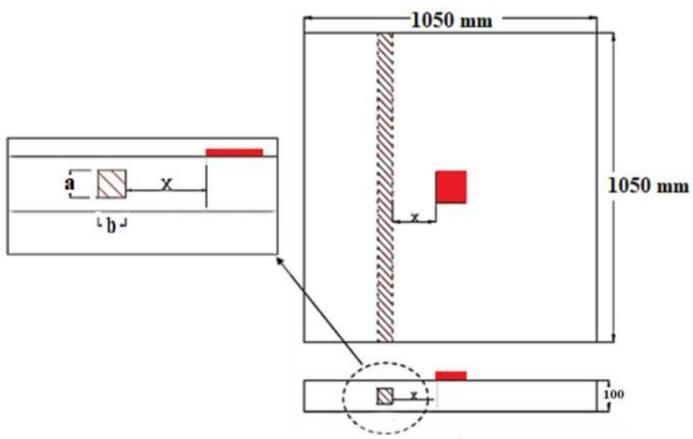

Figure 2. Geometry of duct

Table 1. Tested specimens with their characterized details

Parameters	Specimens	Duct dimension (mm) Duct height (a)	Duct width (b)	Horizontal distance to column face (x) (mm)
Control	S.C	---	---	---
		Group-1		
Distance from column face (x)	S.3.10.0	30	100	0
	S.3.10.5			50
	S.3.10.10			100
		Group-2		
	S.5.10.0	50	100	0
	S.5.10.5			50
	S.5.15.10			100
		Group-3		
Height of duct (a)	S.3.10.0	30	100	0
	S.5.10.0	50		
		Group-4		
	S.3.10.5	30	100	50
	S.5.10.5	50		

Test Setup

As part of this experimental test, the slab specimens were set up on a rigid steel frame with dimensions of 1050 mm x 1050 mm. A steel frame had already been manufactured to accommodate the specimen dimensions and ensure simple support conditions for testing. Every slab specimen has been tested using a hydraulic jack possessing a peak load of 2000 kN. The load has been subjected to the steel plate located on the middle upper face of the slab specimens. It had dimensions of 100 mm x 100 mm and a thickness of 20 mm, laser-cut fabricated to guarantee accuracy in dimensions. This concentrated load, simulating a column load, is exerted centrally on the steel plate and then transferred over the slab. The load was applied at incremental rates of 5 kN, and the corresponding deflection was measured and documented at each step to track the response of the specimens under loading. A dial gauge was placed on a steel plate welded to the steel frame beneath the slab tension surface. The dial gauge was set at the middle span lengths to record the deflections. During loading, the propagation of cracks was also traced by drawing their path lines on the bottom face of the slab specimen. (Figure 3) portrays the test apparatus and the dial gauge instrument.

Figure 3. Test setup

Materials

The cement used for casting the specimens is ordinary Portland cement and conforms to Iraqi Standard Specifications, I.Q.S. No. 5, 2019 (IQS, 2019). In mixes, fine aggregate is sieved to achieve a maximum particle size of 4.75 mm. The physical, chemical, and gradational characteristics of the fine aggregate were specified by Iraqi Standard 45/1984 Locally available gravel was used as the coarse aggregate, sieved to a size range of 5 mm to 14 mm and a gradation that meets the requirements of Iraqi Specification No. 45/1984 for Zone II (IQS, 1984). A steel bar with a diameter of 10 mm was used to reinforce the tested slab specimen in the tension regions. A tensile test was conducted on at least three specimens taken from the steel reinforcement bars used in the tested beams according to ASTM A615-16 specifications (ASTM International, 2016). The characteristics of the reinforced bar that emerged from the test are listed in (Table 2). Hyperplast PC260 is considered a high-performance superplasticizer. It was adopted in the present work for all tested specimens and conforms to the requirements of ASTM C494-17, which was published in 2018 (ASTM International, 2018).

Table 2. Properties of steel reinforcement.

Bar Diameter (mm)	Yield Strength (MPa)	Ultimate Strength (MPa)	Elongation (mm)	ASTM Requirements			
				Grade	Min Yield Strength (MPa)	Min Ultimate Strength (MPa)	Min Elongation
&10	522	647	10.8	60	420	620	9 (for bars from 10 mm to 20 mm)

Mix Design, Fresh, and Mechanical Properties

Integrating chemical admixtures, particularly superplasticizers, a carefully controlled low water-to-cement ratio, and an increased cement amount fundamentally influence the formulation of high-strength concrete mixes. This advanced approach demands a more intricate process than typically used for designing conventional normal-strength mixtures. Therefore, several attempts were made at the beginning of the current study to create mixes and carefully identify the optimum combinations, aiming to achieve the desired strength characteristics. The experiments revealed that the mix proportion of self-compacting high-strength concrete (SCHSC), which outlined in (Table 3), satisfies the requirements of workability and mechanical properties (compressive strength). The fresh properties of the self-compacting concrete (SCC) mix were evaluated by conducting a series of standard tests according to the guidelines of the "European Federation of National Associations Representing Producers and Applicators of Specialist Building Products for Concrete" (EFNARC) (EFNARC, 2002a). The selected tests included the slump flow (EFNARC, 2005), T500 time (EFNARC, 2005), and G-ring test (American Concrete Institute, 2007), which are widely used to recognize and assess the key rheological characteristics of SCC: flowability, viscosity, and passing ability, respectively. These parameters are considered critical to ensure the mix can adequately fill formwork and pass-through reinforcement without requiring mechanical compaction, while maintaining homogeneity and resisting segregation. The results of these tests are compared against the EFNARC-recommended performance limits (EFNARC, 2002b) to confirm the suitability of the mix design for practical application. The findings of the fresh characteristics' tests are presented in (Table 4).

Table 3. Mix the proportion of concrete.

Material	Quantity (kg)	w/c	w/b
Cement	498	0.26	0.236
Water	129		
Fine Aggregate	627		
Coarse Aggregate	1100		
Silica fume	49		
Superplastizer	9.6		

Table 4. Fresh properties test results

Test Type	Results	Limits (according to EFNARC) [35]
Slump Flow	690 mm	(650-800) mm
T_{500}	3.6 sec	(2-5) sec
G-ring	7.8 mm	(0-10) mm

To assess the hardened mechanical performance of the concrete mix, compressive strength (British Standards Institution, 1989), splitting tensile strength (ASTM International, 2017), and flexural (rupture) (ASTM International, 2015) strength tests were carried out on three representative samples. These tests are essential for evaluating the material's capacity to resist axial compression, indirect tension, and flexural stresses, respectively. The average values obtained from the three samples for each characteristic reflect the typical performance of the mix. The outcomes of hardened properties tests are outlined in Table 5.

Results and Discussion

Experimental Results and Performance Metrics

All slab specimens were loaded up to failure. The load was logged over each increment to obtain the relation between load and mid-span vertical displacement. The cracking load, load capacity, and ultimate deflection were obtained from recorded data, while the service deflection and toughness were calculated based on these values.

Table 5. Mechanical properties of mixes used in the tested beams

Test Type	Results			
	Sample-1	Sample-2	Sample-3	Average
Compressive Strength (MPa)	110	103	102	105
Tensile Strength (MPa)	4.55	4.76	4.85	4.72
Rupture Strength (MPa)	8.52	8.61	8.78	8.64

To evaluate the service performance of the slab specimens, a reference service load equivalent to 65% of the ultimate load of the control specimen (0.65Pu of S.C) was used in all slab specimens (Wang et al., 2018). The corresponding mid-span deflections were compared. This approach allowed direct comparison of deformation behavior across various duct configurations. Toughness refers to a material's capacity to absorb energy before fracture and was quantified in this study. The toughness evaluation was performed by calculating the area under the load–deflection curve, derived from the experimental data, as recommended in the manuscript (Barr et al., 1996). (Table 6) demonstrates the outcomes and all necessary calculated data for each tested slab specimen. All specimen failed by punching shear as shown in Figure 4.

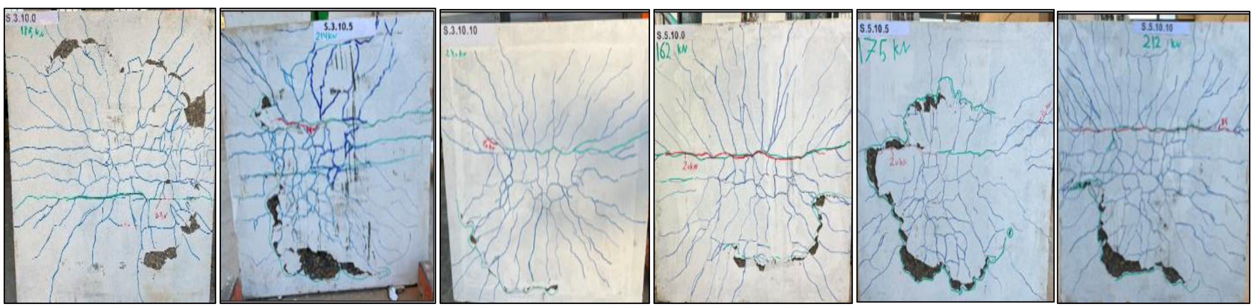

(a) (b) (c) (d) (e) (f)

Figure 4. Crack pattern of bottom face for tested specimens: (a) S.3.10.0, (b) S.3.10.5, (c) S.3.10.10, (d) S.5.10.0, (e) S.5.10.5, (f) S.5.10.10

Table 6. Result of the test and calculated data

Specimens	Cracking Load (kN)	Service Load (0.65Pu) of SC (kN)	Service Deflection (Δs) (mm)	Ultimate Load (kN)	Ultimate Deflection (mm)	Toughness (kN.m)
S.C	80	182	5.12	280	10.46	1.823
S.3.10.0	20	182	6.30	185	6.49	0.704
S.3.10.5	40	182	7.32	214	11.27	1.651
S3.10.10	60	182	5.32	240	8.03	1.162
S.5.10.0	20	Failed	---	162	11.51	1.302
S.5.10.5	20	Failed	---	175	8.36	0.871
S.5.10.10	35	182	7.64	212	11.74	1.633

Parametric Study

Distance from Column Face (x)

1) *Effect of Duct Location on Punching Shear for Group One with a Duct of 30 × 100 mm*

Based on the current group of slab specimens, the effect of the horizontal distance between the duct and the column face was examined, utilizing a duct size of 30 mm × 100 mm. Due to the existence of the duct within the slab thickness, there has been a reduction in load and toughness. In the final loading stage, the effect of the duct's presence intensified and became more prominent and noticeable as the duct grew closer to the column face. The maximum load was lowered by about 33.9%, 23.6%, and 14.3% for distances of 0, 50, and 100 mm, respectively, compared to the (S.C) reference specimen. (Figure 5) demonstrates load-to-mid-span deflection curves for all slab specimens in the current group.

An increasing tendency in service deflection is observed as the duct is positioned farther from the column face. Specimen S.3.10.0, with the duct located directly adjacent to the column, exhibited a 23% increase in service deflection relative to the control. As the duct was moved to 50 mm in specimen S.3.10.5, the deflection increase rose to 43.0%, likely due to interference with critical stress paths. However, positioning the duct at 100 mm in specimen S3.10.10 resulted in only a slight increase of 3.8%, indicating that strategic placement of ducts away from stress concentration zones can preserve serviceability and limit mid-span deformation. (Figure 6) shows the influence of distance from the column face on service deflection.

The observed reduction in slab capacity can be attributed to ducts, which effectively diminish the section area that can carry load transfer and alter the distribution of internal shear stress. This effect was evident near the column face, where high stress concentrations likely contributed to increased vulnerability to punching shear failure. In contrast, their impact was less significant when ducts were positioned farther from the column, perhaps due to less localized stresses in those regions. Moreover, the influence was also notable at the cracking stage because the slab primarily depends on its uncracked concrete section to resist bending in the initial loading phase. The slab generally bends under load, generating the first cracks on its lower surface, mainly in the region farthest from the column. Bending cracks emerge sooner, followed by shear cracks that appear afterward. Therefore, a duct inside the thickness of the slab significantly affects the cracking stage.

It was found that slab specimens containing duct had decreased toughness values compared to solid specimens. In particular, this effect was more pronounced at the column face and 100 mm from it, with decreases of 61.4% and 36.3% in the same sequence. A lower drop in toughness was observed at the S.3.10.5 specimen, 50 mm towards the column face, by around 9.4%. This could explain the increased deflection and the minor drop in toughness compared to the other two locations. (Figure 7) demonstrates the relative impact of the existence of the duct versus the slab reference specimen across three distances from the column face. Based on comparisons with the hollow slab specimen (S.3.10.0), the load capacity was 15.7% higher at 50 mm and 29.7% higher at 100 mm. Likewise, toughness was enhanced by 134.7% and 65.1% for distances 50 mm and 100 mm higher than the slab specimen (S.3.10.0). It was evident that the distance from the column face had a decreasing impact.

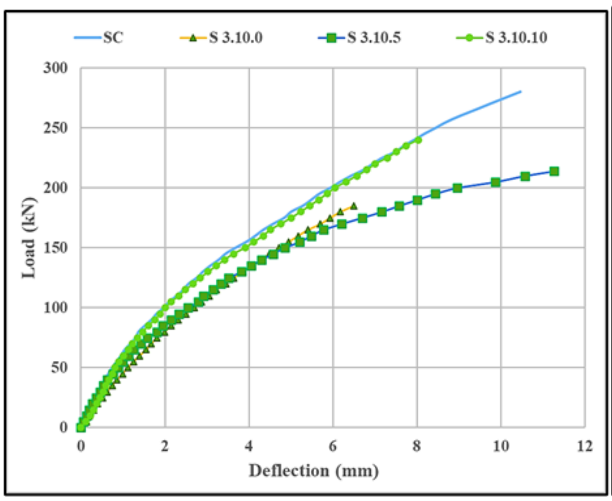

Figure 5. Load-mid span vertical displacement of specimens in for slabs with a duct of 30 × 100 mm

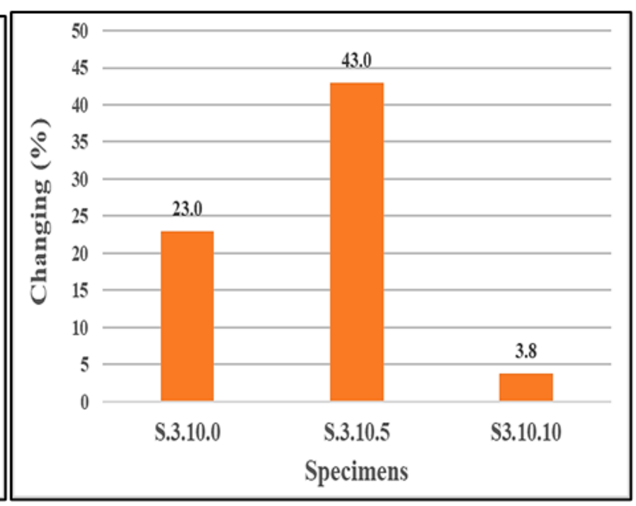

Figure 6. The influence of distance from the column face on service deflection compared to the **S.C.** specimen for slabs with a duct of 30 × 100 mm

2) *Effect of Duct Location on Punching Shear for Group Two with a Duct of 50 mm × 100 mm*

The second group of slab specimens was also constructed to assess the response to the slab specimens with a duct of 50 mm × 100 mm in size at three distinct horizontal distances. The load capacity and toughness revealed a drop in value as a result of the existence of the duct within the slab thickness. When the voided slab specimen reached the final loading stage, the result data confirmed that the most significant influence on the presence of duct was at the face of the column, which tended to decrease away from the face. Depending on the distance between the duct and the column face of 0, 50, and 100 mm, the load capacity was diminished by around 42.1%, 37.5%, and 24.3% compared to the control solid specimen S.C, respectively. (Figure 8) reveals the load-mid span deflection curves for each slab specimen in this group.

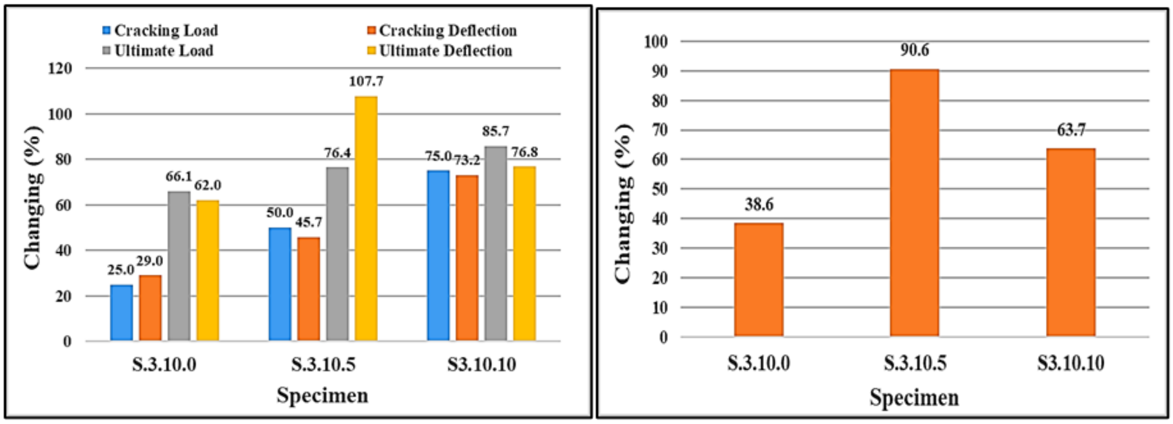

(a) (b)

Figure 7. Relative effect compared to the **S.C** specimen for slabs with a duct of 30 × 100 mm; (a) on load and deflection, (b) on toughness

Both specimens (S.5.10.0 and S.5.10.5) failed before reaching the service load of the control specimen, S.C. Only the specimen S.5.10.10 reached its service deflection of 7.6 mm, achieving a 49.2% increase relative to the control specimen S.C. A comparison of slab specimens with a control solid specimen indicated a notably lower toughness of slab specimens.

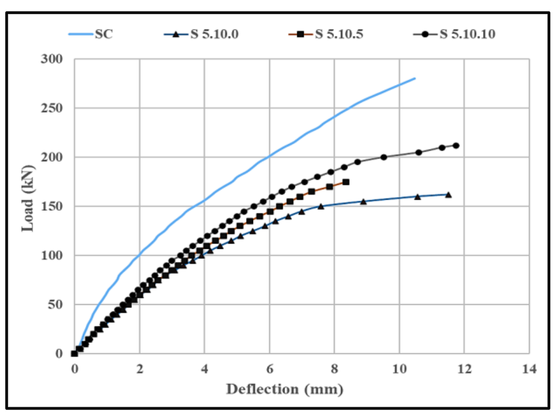

Figure 8. Load-mid span vertical displacement of specimens in for slabs with a duct of 50 × 100 mm

The toughness in the specimen (S.5.10.5) with the duct spaced 50 mm from the column face dropped to approximately 52.2%, followed by the specimen (S.5.10.0) at the column face with 28.5%. The effect was less influential in the (S.5.10.10) specimen, which had a 100 mm distance between the duct and the face of the column, with an approximate drop of 10.4%. There was a negative impact of the duct on the energy dissipation of the slab, despite a slight rise in mid-span deflection of the slab specimen at 0 and 100 mm, since the area under the curve does not depend on deflection value but also on load. The presence of ducts within the slab compromises its toughness and load capacity due to a change in the flow of internal shear stresses. Most of this effect can be observed near the column face under the highest stress level. However, a duct positioned further away from the column is less likely to have an adverse effect because the sharpness of local stress is decreased. Figure 9 demonstrates the relative impact of the existence of the duct compared to the slab control specimen along three distances from the column face.

In the early loading phase, the slab primarily relies on the uncracked concrete section to resist bending, resulting in a prevalence of cracking during the initial cracking stage due to the presence of the duct. Flexural cracking commonly develops at the earliest due to the formation of tensile stresses on the slab's bottom surface when loaded, primarily far from the column support. Unlike shear cracks, bending-induced cracks begin earlier. Shear cracks form when loading increases and shear stress reaches critical levels. Accordingly, the proximity of a duct inside the slab thickness profoundly affects the cracking mechanism, as the stress distribution could be changed, triggering crack initiation at a lower load level.

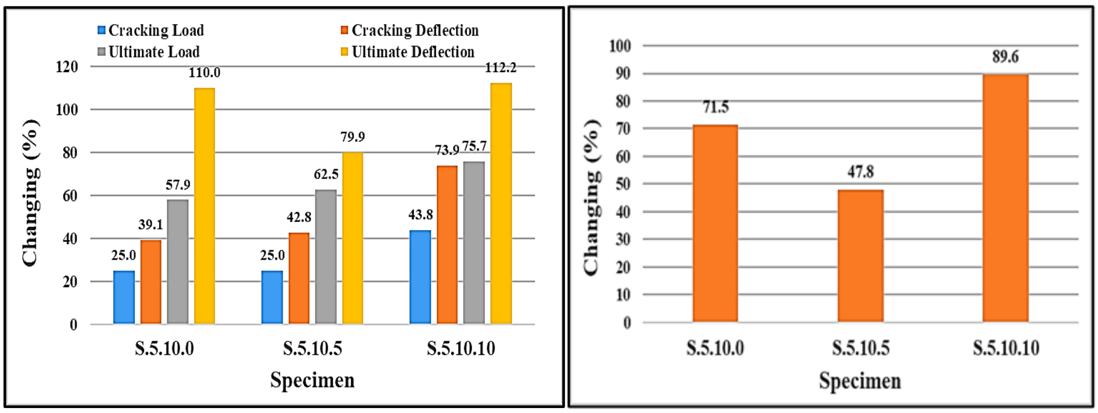

(a) (b)

Figure 9. Relative effect compared to the **S.C** specimen for slabs with a duct of 50 × 100 mm; (a) on load and deflection, (b) on toughness

Based on comparisons with a slab specimen with ducts (S.5.10.0), the ultimate load improvement at a distance of 50 mm was 30.9% and 8% at 100 mm from the column face. The toughness for specimens (S 5.10.5) and (S 5.10.10) recorded a different performance versus the slab specimen with ducts (S.5.10.0). The (S 5.10.5) specimen with a closer duct to the column face (50 mm) showed lowered toughness by about 33.1%. In comparison, the (S 5.10.10) specimen with a farther duct to the column face (100 mm) revealed an increase of around 25.4%. The closer the duct is to the column face, the greater the adverse impact on toughness due to localized failures and reduced structural continuity. A farther duct location mitigates this impact, leading to improved toughness.

Height of Duct (a)

1) *Influence of Duct Height on Load Capacity and Deflection for Group Three (b=100 mm and x= 0mm)*

This group of slab specimens was constructed to investigate the shear behavior of punching for a slab with two duct height values of 30 and 50 mm. All specimens with a duct were chosen to be at the face of the column. When increasing the height of the duct in slab specimens, it was discovered that the failing load dropped in response to this increase from 33.9% for specimen S3.10.0 (with 30 mm duct height) to 42.1% for specimen S5.10.0 (with 50 mm duct height), compared to control solid slab specimen (S.C). (Figure 10) illustrates the curves of load-to-mid deflection for slab specimens in a ninth group.

Specimen S.3.10.0 exhibited a 23 % increase in mid-span deflection under the service load compared to the control specimen S.C, indicating a moderate reduction in flexural stiffness due to the presence and height of the duct. In contrast, specimen S.5.10.0, which possesses a higher height, cannot carry the designated service load (65% of the ultimate load of the control specimen). Hence, this suggests that the slab specimen failed before reaching the service load threshold, likely due to its larger duct height. The specimen with a duct height of 50 mm exhibited weaker stiffness due to the presence of the larger duct. Therefore, it produced greater deflection, even in the early loading stage, which made the toughness seem larger. Figure 11 revealed the relative influence of the duct height compared to the solid slab control specimen (S.C) based on two distinct duct heights. Based on comparing the results, the ultimate load values were compared against the specimen with a smaller duct height (S3.10.0 specimen), and a drop was noted, reaching 12.4%.

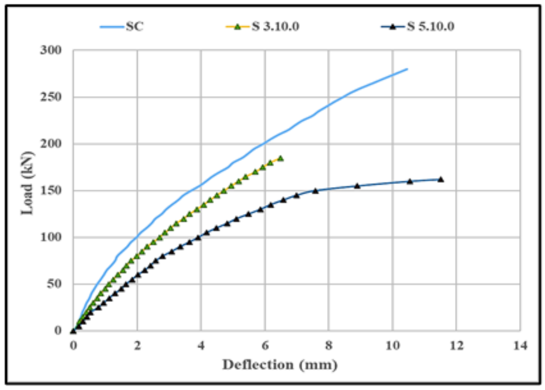

Figure 10. Load-mid span vertical displacement of specimens for slabs with b= 100 mm and x=0

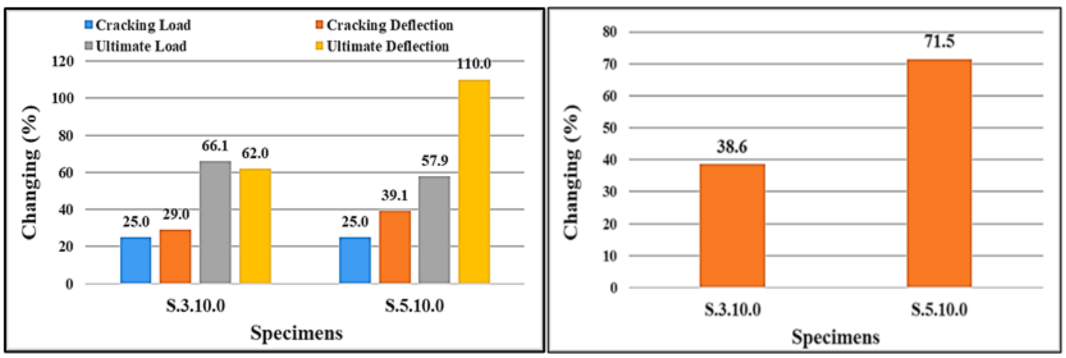

(a) (b)

Figure 11**.** Relative effect compared to the S.C specimen for slabs with b= 100 mm and x=0; (a) on load and deflection, (b) on toughness

The observed reduction in failure load with increasing duct height can be attributed to the vertical interruption of the concrete cross-section, which significantly affects the ability of the slab to resist flexural and punching shear forces. As the duct height increases, this limits the ability of the slab to transfer shear stresses since punching shear resistance in slabs is highly dependent on the perimeter of the critical section and the effective depth. The reduction in deflection for the specimen with a 30 mm duct height suggests a more brittle response, likely due to early cracking and reduced post-crack toughness.

2) Influence of Duct Height on Load Capacity and Deflection for Group Four (b=100 mm and x= 50mm)

An evaluation of punching behavior was performed on slab specimens with 30 mm and 50 mm duct heights located 50 mm from the face of the column. It was observed that the maximum load decreased as duct height grew in slab specimens, where the lowering in the ultimate load was 23.6% in a specimen containing a duct height of 30 mm (namely S3.10.5) and it became 37.5% for a specimen containing a duct height of 50 mm (namely S5.10.5), relative to control solid slab specimen (S.C). (Figure 12) illustrates the load-to-mid vertical displacement in the current group of slab specimens. Specimen S.3.10.5 exhibited a 43% increase in mid-span deflection under service load compared to the control specimen S.C, reflecting a significant reduction in flexural stiffness. This behavior is attributed to the impact of the presence of the duct and its height. Meanwhile, specimen S.5.10.5, which had a greater duct height, failed to meet the original service load limitation of the control specimen. Consequently, increasing the duct height can seriously compromise the slab, impairing its ability to satisfy service demands for a reference slab that lacks a duct.

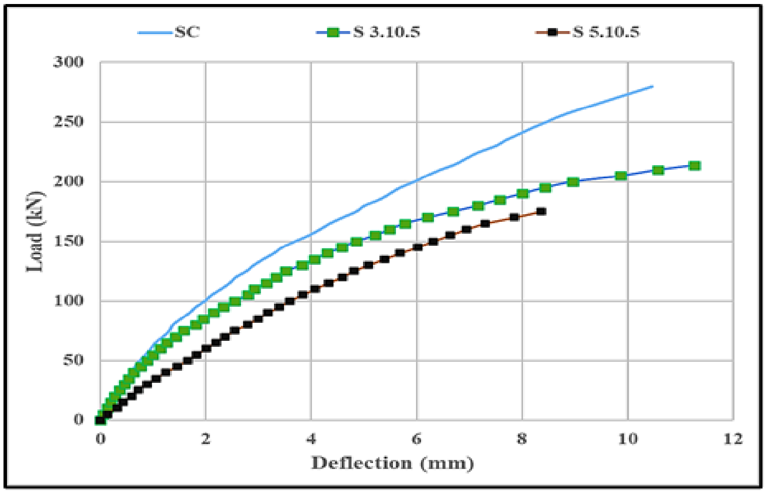

Figure 12. Load-mid span vertical displacement of specimens for slabs with b= 100 mm and x=50 mm

The value of toughness in a specimen containing a larger duct height was also demonstrated, where the most pronounced drop in toughness occurred; subsequently, in a specimen containing a smaller duct height. Thus, it can be seen that the toughness of specimens S3.10.5 decreased by approximately 9.4% and by about 52.2% in the S5.10.5 specimen versus the control solid slab specimen (S.C). (Figure 13) demonstrates the relative effect of the duct height compared to the solid slab control specimen (S.C) in terms of two different duct heights.When the load capacity and toughness findings were compared to those of the specimen with a smaller duct height (S3.10.5), the load capacity and toughness values fell to 18.2% and 47.2% for the same sequence of specimens. The observed decline in maximum load with increasing duct height in slab specimens is consistent with structural behavior where internal voids disrupt the continuity of the load-carrying concrete section. As duct height increases, the effective depth of the slab is reduced. This results in lower shear strength and, thus, reduced load-bearing capacity. The reduction in toughness is more severe in the specimen with a larger duct height (S5.10.5), which confirms that increasing the vertical height of voids significantly compromises the slab's energy absorption capacity. The reduced amount of concrete material in critical stress paths due to larger voids limits the specimen's capacity to resist progressive cracking and deformation. Moreover, larger voids are associated with more localized stress concentrations and earlier onset of critical cracking, leading to premature failure and reduced post-peak performance. When comparing the performance of the specimen with the larger duct height S3.10.5 against the one with the smaller duct height, there is a clear degradation in both load capacity and toughness, emphasizing that as the duct height increases, both strength and energy dissipation abilities deteriorate significantly. The sharp decline in toughness suggests a weaker but also more brittle structure, with a steeper loss of capacity after peak load.

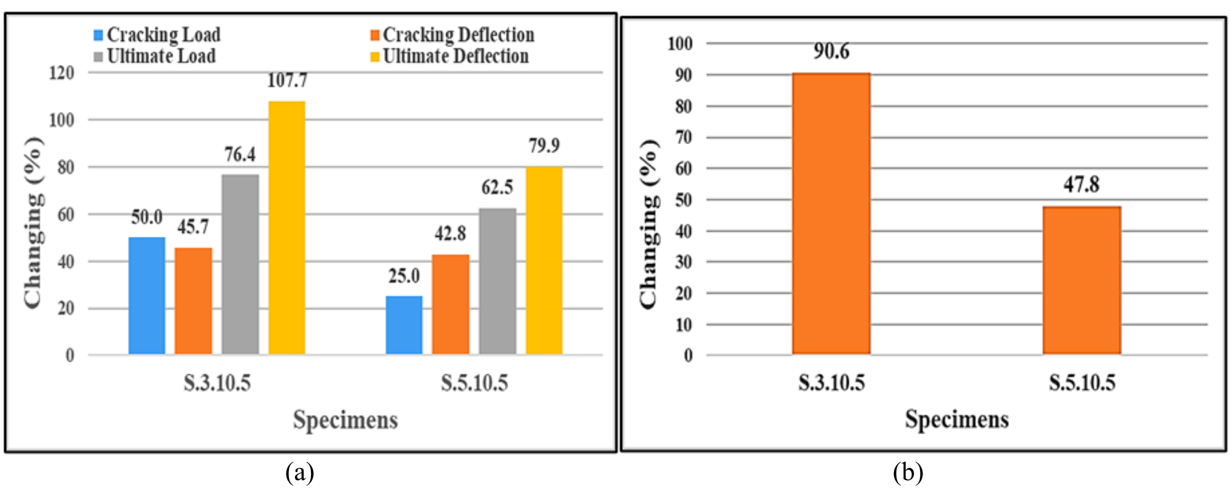

Figure 13. Relative effect of duct height compared to the S.C specimen for slabs with b= 100 mm and x=50 mm; (a) on load and deflection, (b) on toughness.

Conclusion

Several discernible conclusions have been drawn from the present study, which can be summarized in the following points:

Slab specimens constructed with a 30 mm × 100 mm duct exhibited notable changes in shear performance, particularly as the duct was placed closer to the column face. The ultimate load capacity showed its most significant reduction up to 33.9% when the duct was located directly at the column face, with progressively smaller decreases observed at increased distances Toughness was most severely reduced at the 0 mm position, with a 61.4% drop. A duct positioned at the column face impaired the shear performance of slab specimens with a 50 mm × 100 mm duct, with the worst loss in load capacity reaching 42.1%. Serviceability was severely affected at 0 mm and 50 mm, where the failure occurred before reaching the service load. Toughness was significantly reduced, with the sharpest decline of 52.2%.

The ducts with a constant width of 100 mm were placed at the column face, and it was found that increasing the duct height from 30 to 50 mm had an adverse effect on shear performance. After the duct height increased, the reduction in ultimate load capacity grew worse, from 33.9% to 42.1%. The specimen with a 30 mm duct height exhibited a 23% increase in mid-span service deflection, inferring moderate stiffness loss. In addition, the specimen with a 50 mm duct height could not comply with the service load requirement.

Slab specimens incorporating a 100 mm wide duct located 50 mm from the column face exhibited an apparent reduction in performance as the duct height rose. The specimen with a smaller duct height experienced a 23.6% drop in ultimate load capacity, indicating a lesser effect than the specimen with a larger duct, which experienced a 37.5% decline in load capacity. Serviceability declined with increasing duct height; the 30 mm duct specimen had a 43% rise in deflection, reflecting diminished stiffness, while the 50 mm duct specimen could not carry the service load limit as in the control specimen, reflecting a severe loss in stiffness. Toughness also declined with increasing duct height, dropping modestly in the specimen containing a 30 mm duct but reaching a substantial lowering of 52.2% in the specimen containing a 50 mm duct. These results confirm that greater duct height, even when placed slightly away from the column face, severely impairs load-bearing capacity and service-level performance.

The influence of duct presence was also notable at the cracking stage because the slab primarily depends on its uncracked concrete section to resist bending in the initial loading phase. The slab generally bends under load, generating the first cracks on its lower surface, mainly in the region farthest from the column. Bending cracks emerge sooner, followed by shear cracks that appear afterward. Therefore, a duct inside the thickness of the slab significantly affects the cracking stage.

The observed reduction in slab capacity can be attributed to ducts, which effectively diminish the section area that can carry load transfer and alter the distribution of internal shear stress. This effect was evident near the column face, where high stress concentrations likely contributed to increased vulnerability to punching shear failure. In contrast, their impact was less significant when ducts were positioned farther from the column, perhaps due to less localized stresses in those regions.

Practical Recommendations

Based on the outcomes and conclusions of the present study, the following practical notes may be recommended for engineers or future work: It is preferable to embed the duct at a distance not less than the slab thickness far away the column edge to avoid interrupting the flow of internal shear forces. Acceptable duct height should be lesser than 1/3 the slab thickness to reduce the diminished section area that can carry load transfer. It is recommended to increase the shear strength of the slab around the ducts using internal shear reinforcement or external strengthening techniques.

Scientific Ethics Declaration

* The authors declare that the scientific ethical and legal responsibility of this article published in EPSTEM journal belongs to the authors.

Funding

* This research received no specific grant from any funding agency in the public, commercial, or not-for-profit sectors.

Conflict of Interest

* The authors declare that they have no conflicts of interest.

Acknowledgements or Notes

* This article was presented as an oral presentation at the International Conference on Engineering and Advanced Technology (ICEAT) held in Selangor, Malaysia on July 23-24, 2025.

References

ACI Committee 237. (2007). *Self-consolidating concrete* (ACI 237R-07). American Concrete Institute.

Al-Bahrani, A. I., & Al-Tameemi, H. A. (2025a). Two-way shear behaviors in hybrid flat slabs with inset circular ducts. *AIP Conference Proceedings*, *3292*(1), 060005.

Al-Bahrani, A. I., & Al-Tameemi, H. A. (2025b). Two-way shear behaviors in hybrid reinforced concrete flat slabs with inset square ducts. *AIP Conference Proceedings*, *3292*(1), 060004.

Al-Quraishi, H. A. (2014). *Punching shear behavior of UHPC flat slabs* (Doctoral dissertation). University of Kassel.

Al-Tameemi, H. A., Habelalmateen, M. A., & Alalikhan, A. A. (2021). Effect of embedded pipelines within slab thickness on punching shear capacity of flat slabs. *KSCE Journal of Civil Engineering*, *25*(1), 208-218.

ASTM International. (2015). *Standard test method for flexural strength of concrete (using simple beam with third-point loading)* (ASTM C78/C78M-15).

ASTM International. (2016). *Standard specification for deformed and plain carbon-steel bars for concrete reinforcement* (ASTM A615).

ASTM International. (2017). *Standard test method for splitting tensile strength of cylindrical concrete specimens* (ASTM C496/C496M-17).

ASTM International. (2018). *Standard specification for chemical admixtures for concrete* (ASTM C494).

Barr, B., Gettu, R., Al-Oraimi, S. K. A., & Bryars, L. S. (1996). Toughness measurement—the need to think again. *Cement and Concrete Composites*, *18*(4), 281-297.

British Standards Institution. (1989). *Method of determination of particle size distribution* (BS 812: Part 103).

Dhavale, N. K., & Fayaz, I. U. (2019). Planning, design & analysis of a commercial building with flat slab considering earthquake induced forces using ETABS. *International Journal of Engineering Research and Application*, *6*(11), 396-412.

EFNARC. (2002). *Specification and guidelines for self-compacting concrete*. Association House, 99 West Street, Farnham, Surrey GU9 7EN, UK.

EFNARC. (2005). *The European guidelines for self-compacting concrete: Specification, production and use*. https://www.theconcreteinitiative.eu/images/ECP_Documents/EuropeanGuidelinesSelfCompactingConcrete.pdf

El-Mawsly, E. H., El-Kashif, K. F. O., Shawky, A. A., & Abdalla, H. A. (2022). Experimental and numerical investigation on strengthening of RC flat slabs with central opening. *Case Studies in Construction Materials*, *16*, e00974.

Faria, R., Marreiros, R., Ramos, A. P., & Jesus, C. (2020). Influence of the top reinforcement detailing in the behaviour of flat slabs. *Structures*, *23*, 718-730.

Ghannoum, C. M. (1998). *Effect of high-strength concrete on the performance of slab-column specimens*. *ACI Structural Journal 95*(S21), 227.

Ghayeb, H. H., Atea, R. S., Al-Kannoon, M. A. A., Lee, F. W., Wong, L. S., & Mo, K. H. (2023). Performance of reinforced concrete flat slab strengthened with CFRP for punching shear. *Case Studies in Construction Materials*, *18*, e01801.

Hanson, J. M. (1970). *Influence of embedded service ducts on strength of flat-plate structures*. Portland Cement Association.

Hassoun, M. N., & Al-Manaseer, A. (2020). *Structural concrete: Theory and design*. John Wiley & Sons.

Iraqi Organization of Standards. (1984). *Aggregates from natural sources for concrete and building construction* (IQS No. 45).

Iraqi Organization of Standards. (2019). *Portland cement* (IQS No. 5).

Kamonna, H. H., Shakir, Q. M., & Al-Tameemi, H. A. (2020). Behavior of high-strength self-consolidated reinforced concrete T-deep beams. *The Open Construction & Building Technology Journal*, *14*(1). DOI: 10.2174/1874836802014010051

Kolapuri, A., Ashwin, P., & Siddardha, K. (2018). Construction of flat slabs. *International Journal of Innovative Research in Science, Engineering and Technology*, *7*(5), 4866-4873.

Lapi, M., Ramos, A. P., & Orlando, M. (2019). Flat slab strengthening techniques against punching-shear. *Engineering Structures*, *180*, 160-180.

Lee, J. H., & Yoon, Y. S. (2010). Prediction of strength of interior HSC column–NSC slab joints. *Magazine of Concrete Research*, *62*(7), 507-518.

Mehdi, W. S., & Al-Tameemi, H. A. (2024a). Effect of embedded square ducts on two-way shear capacity of lightweight concrete flat slabs. *AIP Conference Proceedings*, *3249*(1), 020011.

Mehdi, W. S., & Al-Tameemi, H. A. (2024b). Punching shear capacity of lightweight concrete flat slabs with embedded pipelines. *AIP Conference Proceedings*, *3249*(1), 020008.

Metwally, I. M., Issa, M. S., & El-Betar, S. A. (2008). Punching shear resistance of normal and high strength reinforced concrete flat slabs. *Civil Engineering Research Magazine*, *30*(3), 982-1003.

Olmati, P., Sagaseta, J., Cormie, D., & Jones, A. E. K. (2017). Simplified reliability analysis of punching in reinforced concrete flat slab buildings under accidental actions. *Engineering Structures*, *130*, 83-98.

Rashid, M. A., & Mansur, M. A. (2009). Considerations in producing high strength concrete. *Journal of Civil Engineering (IEB)*, *37*(1), 53-63.

Said, M., Adam, M. A., Arafa, A. E., & Moatasem, A. (2020). Improvement of punching shear strength of reinforced lightweight concrete flat slab using different strengthening techniques. *Journal of Building Engineering*, *32*, 101749.

Shannag, M. J. (2000). High strength concrete containing natural pozzolan and silica fume. *Cement and Concrete Composites*, *22*(6), 399-406.

Shatarat, N., & Salman, D. (2022). Investigation of punching shear behavior of flat slabs with different types and arrangements of shear reinforcement. *Case Studies in Construction Materials*, *16*, e01028.

Thiele, C. (2010). *Zum tragverhalten von stahlbetonplatten ohne querkraftbewehrung mit integrierten leitungsführungen* [Doctoral dissertation]. University of Kaiserslautern.

Wang, C., Shen, Y., Zou, Y., Li, T., & Feng, X. (2018). Stiffness degradation characteristics destructive testing and finite-element analysis of prestressed concrete T-beam. *Computer Modeling in Engineering & Sciences*, *114*(1), 75-93.

Yehia, E., Khalil, A. H., Mostafa, E. E., & El-Nazzer, M. A. (2023). Experimental and numerical investigation on punching behavior of ultra-high performance concrete flat slabs. *Ain Shams Engineering Journal*, *14*(10), 102208.

Zhou, F. P., Barr, B. I. G., & Lydon, F. D. (1995). Fracture properties of high strength concrete with varying silica fume content and aggregates. *Cement and Concrete Research*, *25*(3), 543-552.

Author(s) Information

Mohammed Hammed Al-Khazraji
University of Kufa, Najaf, Iraq
Contact e-mail: *mohammedalkhazrgy@gmali.com*

Haider Ali Al-Tameemi
University of Kufa, Najaf, Iraq

To cite this article:

Al-Khazraji, M. H., & Al-Tameemi, H.A. (2025). Impact of duct position on behavior of high-strength reinforced concrete flat slab. *The Eurasia Proceedings of Science, Technology, Engineering and Mathematics (EPSTEM), 37,* 1082-1096.